Measurement of low energy K^+ total cross sections on $N = Z$ nuclei

R. Weiss,[1] J. Aclander,[1] J. Alster,[1] M. Barakat,[3] S. Bart,[2] R.E. Chrien,[2]
R.A. Krauss,[4] K. Johnston,[4] I. Mardor,[1] Y. Mardor,[1] S. May Tal-beck,[1]
E. Piasetzky,[1] P.H. Pile,[2] R. Sawafta,[2] H. Seyfarth,[5] R.L. Stearns,[6] R.J. Sutter,[2]
and A.I. Yavin[1]

[1] *School of Physics, Raymond and Beverly Sackler Faculty of Exact Sciences, Tel Aviv University, Tel Aviv 69978, Israel*
[2] *Brookhaven National Laboratory, Upton New York 11973*
[3] *University of Houston, Houston, Texas 77204*
[4] *Texas A&M University, College Station, Texas 77843*
[5] *KFA, Jülich, Germany*
[6] *Vassar College, Poughkeepsie, New York, 12601*

(Received 10 December 1993)

The total cross sections for K^+ on deuterium, ^{6}Li, ^{12}C, ^{28}Si, and ^{40}Ca have been measured at four-momenta in the range 480–714 MeV/c. The experimental technique was of the standard transmission type. Because of its long mean free path in nuclear matter at low energies the K^+ can be expected to probe the entire volume of the nucleus. Indeed we found that, to better than 10%, $\sigma(K^+A) = A\sigma(K^+N)$ up to $A = 40$. This feature was used to study more delicate effects of the nuclear medium. Special emphasis was placed on measuring the total cross section ratios of K^+A to K^+D with a precision of $\leq 2\%$. This ratio is a good measure of nuclear medium effects because many experimental as well as theoretical systematic uncertainties cancel in the ratio. We discuss the medium dependence as a function of A. The data do not agree with calculations which include only conventional medium effects. This points towards the need of unconventional nuclear medium effects such as partial quark deconfinement, mass rescaling of nuclear pionic fields, or pion excess in nuclei. Thus far only calculations based on unconventional medium effects for ^{12}C exist. Calculations for the other nuclei are needed before quantitative conclusions can be drawn.

PACS number(s): 25.80.Nv, 21.65.+f, 24.85.+p

I. INTRODUCTION

Among the hadronic probes, the K^+ holds a very special position. Below 1 GeV/c, the K^+N strong interaction has a slow energy and momentum dependence and is the weakest of all strong-interaction processes [1]. The typical K^+N cross section (which is 10 mb on the average) is much smaller than the πN and K^-N cross sections in the same momentum region. The implication for K^+-nucleus scattering is significant. A small cross section means a long mean free path ($\lambda = \frac{1}{\rho\sigma} > 5$ fm) for propagation of the K^+ in the nuclear medium. Therefore the low-momentum K^+ is capable of probing a large part of the nuclear volume, in contrast to the strongly interacting particles which get absorbed at the surface.

Indeed, to first order, the low-momentum K^+-nucleus interaction can be viewed as a single scattering of the K^+ with a nucleon in the nucleus. About 90% of $\sigma(K^+$-^{12}C) is due to single scattering and 98% to single plus double scattering [2]. Thus, only small and calculable corrections to this picture are needed. Within the classical picture of unchanged nucleons in the nucleus, the K^+ interaction with the nucleus can be constructed from the K^+N interaction with much greater reliability than for any other strongly interacting nuclear probe. One of the purposes of this experiment is to test this expectation.

We measured the total cross sections of K^+ on several nuclei in the momentum range 480–714 MeV/c using the fact that these properties of the K^+ make it an ideal probe to study various aspects of the strong interaction and nuclear structure. In particular, one can study the possible changes of the nucleon structure in the nucleus by measuring the ratio

$$R_T \equiv \frac{\sigma_{\rm tot}(K^+\text{-nucleus})/A}{\sigma_{\rm tot}(K^+\text{-deuteron})/2} \ . \tag{1}$$

This ratio, in the approximation of negligible deuteron binding, represents the cross section with respect to a free-space isospin average. Our earlier measurement of K^+-^{12}C and K^+D interactions in the same momentum range, reported by Krauss *et al.* [3], shows that the experimental ratios R_T lie considerably above the predictions of Siegel *et al.* [2] and of Chen and Ernst [4] that are based on free-space K^+N amplitudes.

Siegel *et al.* [2] suggested a deviation from the standard picture. They calculated the K^+-nucleus interaction for carbon with a microscopic optical potential, which incorporates nucleon binding, recoil, and Pauli blocking. We will refer to the latter as "conventional medium corrections." Next, they argued that if the nucleons in the nucleus "swell," the K^+N phase shifts will increase. As a result, the size of the K^+N interaction inside a nucleus will differ from the free one. Brown *et al.* [5] proposed an alternative interpretation based on a density-dependent effective mass of the exchanged mesons in a boson exchange model of the K^+N interaction.

Our earlier carbon results [6], which are consistent with the new data shown in Fig. 1, stimulated the appearance of further calculations, all of which contain "unconventional effects." Caillon and Labarsouque [7] evaluated "unconventional effects" such as the density dependences of nucleon and meson masses and meson-nucleon coupling constants. All three effects raise the values of R_T. In their picture, the meson mass density dependence by itself gives a good description of the data, while the nucleon mass plays a minor role and the coupling constants are not sufficiently well determined to make quantitative statements.

Akulinichev [8] made a rough estimate of the influence of the meson excess in nuclei. Jiang and Koltun [9] calculated the meson exchange current (MEC) contribution to K^+-nucleus elastic scattering using a model of the off-shell $K\pi$ scattering amplitude and a calculation of the excess pion distribution in finite nuclei. They derived both real and imaginary forward-scattering amplitudes for the MEC contribution. Their amplitudes interfere constructively with the optical-model amplitudes and they lead to a momentum-dependent increase in the calculated total cross sections.

The upper bound of the optical-model calculations by Siegel *et al.* [2] are presented in Fig. 1 along with the ^{12}C data of the current experiment. The figures also contain some of the theoretical predictions that include "unconventional" corrections. The upper figure shows the 10% "swelling" calculation [2] (dashed line) and the calculation with density dependence of the exchange meson mass [5] (dot-dashed line). The lower figure has calculations which take into account the pion excess in the nucleus [9] (dotted line) and the density dependences of mesons and nucleons (dashed line) [7]. We concluded that medium effects other than the conventional ones play a role in ^{12}C.

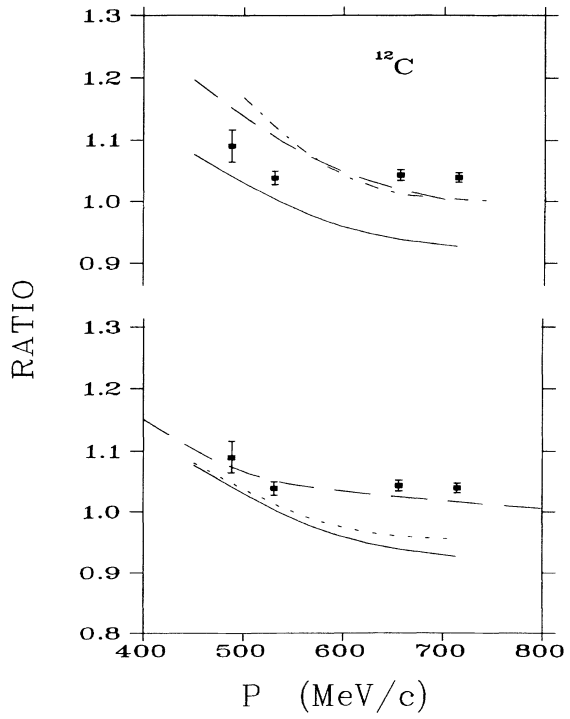

FIG. 1. The calculated ratios R_T by Siegel *et al.* [2] (solid line) and data from this experiment are presented in the upper and the lower figures for ^{12}C. The upper figure includes also the 10% "swelling" calculation by Siegel *et al.* (dashed line) and density meson mass dependence by Brown *et al.* [5] (dot-dashed line). The lower figure includes the calculations for the excess of pions in the nucleus by Koltun [9] (dotted line) and a calculation by Labarsouque (see text) [7] (dashed line).

The purpose of the present experiment is to check whether carbon is unique or whether nonconventional medium effects are a global nuclear feature. The targets were chosen to study a possible nuclear density dependence. We measured the ratios of the total cross sections of K^+ on ^{6}Li, ^{12}C, ^{28}Si, and ^{40}Ca to deuterium with an accuracy of $1-2\%$ in the momentum region of 480–720 MeV/c. We chose $N = Z$ nuclei so that the ratio R_T may be viewed as the isospin-averaged cross section per nucleon in the nucleus relative to the free-space isospin average. One expects a small increase in the ratio for the loosely bound ^{6}Li nuclei and a larger increase for ^{12}C, ^{28}Si, and ^{40}Ca.

The experimental apparatus is outlined in Sec. II while Sec. III describes the data analysis. The error analysis is given in Sec. IV and the results and a discussion appear in Sec. V.

II. EXPERIMENTAL DETAILS

The experiment was performed with the K^+ beam at LESB-II (Low Energy Separated Beam) at the Brookhaven National Laboratory AGS (Alternating Gradient Synchrotron). The measurements were taken at beam momenta (at center of target) of 488, 531, 656, and 714 MeV/c. For each momentum, the beam was tuned to optimize the K to π ratio, the singles rate in the transmission detectors, and the beam phase space at the target. For the various momenta we obtained from 9000 (714 MeV/c) to 4000 (488 MeV/c) kaons in an AGS beam spill of 1.2 s duration every 3 s. The K to π ratio varied with momentum from 1:3 (for 714 MeV/c) to 1:50 (for 488 MeV/c). In all measurements the singles rate on the largest transmission counter was kept below 5×10^5 particles per second.

The experimental apparatus is basically the same as illustrated in our previous paper [3] in Fig. 1 and, except for the omission of the lead collimation, the experimental conditions were virtually identical to those described in [3, 10, 11]. The kaons were identified by a time-of-flight (TOF) system, combined with a differential Cherenkov detector. The probability that a pion was misidentified as a kaon was less than 2×10^{-5}.

A transmission array was used to count the unscattered and forward-scattered particles. It consisted of nine concentric circular plastic scintillators 0.6 cm thick with diameters ranging from 10 to 46 cm. The scintillators were arranged along the beam axis in order of increasing radius, with the first counter at 44 cm from the center of the target. They subtended solid angles ranging from about 42 to 500 msr. A small detector was installed behind the last transmission counter in order to monitor

TABLE I. The targets.

Target	Thickness (mm)	Density $\left(\frac{g}{cm^2}\right)$
Li	43.69	2.09
LiD	25.30	2.02
C	21.69	3.54
CD_2	33.54	3.55
Si	17.11	3.89
Ca	26.00	4.11

the efficiency of each detector in real time. More details are given in Refs. [3], [11], and [12].

The targets, together with an empty frame, were mounted on a target holder and were cycled through the beam at a rate of about 5 min per target. This was done in order to minimize the effect of instabilities. The target details are listed in Table I.

The K^+D total cross sections were measured indirectly by using solid ^{6}LiD and CD_2 targets. Those targets were similar in geometry and energy loss to the solid ^{6}Li and C targets, respectively. This decreased systematic errors in the ratios of Li and C to D total cross sections caused by energy loss and K-decay corrections.

The beam momenta were determined by measuring the TOF of the incoming kaons and they are listed in Table II. We corrected for the energy loss of the kaons on their way into the target, and the momenta at the center of the targets are listed in the table as well.

III. DATA REDUCTION AND ANALYSIS

A complete description of the way in which the total cross sections were extracted from the data was given in [3, 10–12]. We will present just a short summary. Partial transmission cross sections were calculated according to

$$\sigma_{\rm tr}(\Omega_i) = \frac{1}{nt}\ln\left[\frac{R(\Omega_i)_{\rm out}}{R(\Omega_i)_{\rm in}}\right], \tag{2}$$

where nt is the number of scatterers per cm^2, $R(\Omega_i)_{\rm out}$ is defined as the ratio S_i/KB for the empty target run, and $R(\Omega_i)_{\rm in}$ stands for the measurement with the target in place (S_i is the number of counts in the detectors 1 to i, and KB is the number of beam particles).

We followed the prescription of Kaufmann and Gibbs [13] in order to obtain the so-called "Coulomb-free" total cross section by subtracting the integrated Coulomb elastic (c) and Coulomb-nuclear interference (cn) contributions from the measured transmission cross sections ($\sigma_{\rm tr}$). An additional correction was applied by adding the nuclear elastic (n) cross section within the angular range subtended by the transmission counter. The nuclear partial cross sections are then

$$\sigma(\Omega_i) = \sigma_{\rm tr}(\Omega_i) - \sigma_c(>\Omega_i) - \sigma_{cn}(>\Omega_i) + \sigma_n(<\Omega_i). \tag{3}$$

At each momentum we have sets of nine partial cross sections $\sigma(\Omega_i)$ ($i = 1 \ldots 9$), for the six targets: Li, LiD, C, CD_2, Si, and Ca. The deuteron partial cross sections were extracted according to

$$\sigma_{\rm D_{Li}}(\Omega_i) = \sigma_{\rm LiD}(\Omega_i) - \sigma_{\rm Li}(\Omega_i), \tag{4}$$

and

$$\sigma_{\rm D_C}(\Omega_i) = [\sigma_{\rm CD_2}(\Omega_i) - \sigma_{\rm C}(\Omega_i)]/2. \tag{5}$$

These two sets were found to be in good agreement.

The total cross sections [$\sigma_{\rm tot} = \sigma(\Omega = 0)$] were obtained by fitting the partial cross sections to a second-order polynomial in Ω. For the heavy targets, Si and Ca, the Coulomb cross sections are large and dominate the first partial cross section of the measurement and the nuclear-Coulomb correction is highly oscillatory at small angles. Therefore, we omitted the first counter in the fitting procedure using just $\sigma(\Omega_i)$ for $i = 2, \ldots, 9$. We illustrate the problem in Fig. 2 for calcium, where one can see the difference in the fitting results with and without the first detector for 656 MeV/c. For comparison, we also show a fit for the lightest nucleus Li. The 714 MeV/c data were fitted without the ninth partial cross section because their "singles" rates were very high in some cases.

The total cross sections $D_{\rm Li}^{\rm tot}$ and $D_{\rm C}^{\rm tot}$ were obtained from linear fits to the two sets $\sigma_{\rm D_{Li}}$ and $\sigma_{\rm D_C}$. A first-order fit for deuterium was adequate even though the Li, LiD, C, and the CD_2 data required second-order polynomials.

We mention again a few significant corrections which were already discussed in the previous paper [3]. Corrections are made for kaons that decay between the target and the detector array, ($\sigma_{K\text{-decay}}$), and for the contamination of pions and muons which are products of kaons

TABLE II. The momentum at the entrance to the experimental area and the momentum at the center of the target, after momentum loss calculations. Momenta are in units of MeV/c, and nominal momenta for C are used for the ratios.

p ($S1$)	511.9 ± 1.9	553.2 ± 1.2	675.5 ± 1.9	731.2 ± 2.3
Li	490.2 ± 2.4	533.6 ± 1.7	658.2 ± 2.1	716.0 ± 2.4
LiD	490.3 ± 2.4	533.7 ± 1.7	658.2 ± 2.1	716.1 ± 2.4
C	487.7 ± 2.4	531.3 ± 1.7	656.3 ± 2.1	714.3 ± 2.4
CD_2	487.3 ± 2.4	531.0 ± 1.7	656.1 ± 2.1	714.0 ± 2.4
Si	487.6 ± 2.4	531.3 ± 1.7	656.2 ± 2.1	714.2 ± 2.4
Ca	487.5 ± 2.4	531.2 ± 1.7	656.2 ± 2.1	714.1 ± 2.4

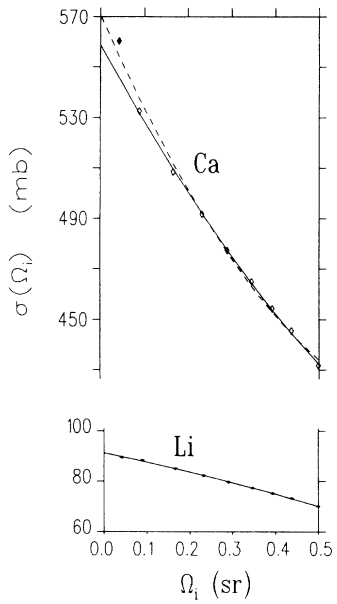

FIG. 2. Partial cross sections for Li and Ca (at 656 MeV/c) with extrapolation to zero solid angle. A comparison is made between the extrapolations for Ca with the first counter (dashed line) and without it (solid line).

that decay downstream from the differential Cerenkov counter and are labeled as kaons by the TOF system, $(\sigma_{\pi\text{-}\mu})$.

A correction is made for target impurities. Enriched Li and natural C, Si, and Ca targets were used. The enriched lithium consisted of 95.59% ^{6}Li and 4.41% ^{7}Li, and the lithium deuteride was 94.5% ^{6}LiD, 4.3% ^{7}LiD, 1.13% ^{6}LiH, and 0.05% ^{7}LiH. The CD_2 target had a contamination of 2.9% $^{12}CH_2$ and 0.03% $^{13}CH_2$. The method for determining the hydrogen content of the CD_2 target was discussed in [3] and [10]. The total cross sections quoted for the $(N = Z)$ isotopes were extracted from the measured cross sections of the natural targets with the very good approximation that the total cross section for some element is proportional to A.

Table III shows the extrapolated cross sections σ_{ext} with the corrections $\sigma_{K\text{-decay}}$, $\sigma_{\pi\text{-}\mu}$, σ_{A^t} (the correction for target impurities), and the final total cross sections σ_{tot}, according to $\sigma_{\text{tot}} = \sigma_{\text{ext}}\text{-}\sigma_{K\text{-decay}} - \sigma_{\pi\text{-}\mu} - \sigma_{A^t}$ for Li, C, Si, and Ca and $\sigma_{\text{tot}} = \sigma_{\text{ext}} - \sigma_{K\text{-decay}} - \sigma_{\pi\text{-}\mu} + \sigma_{A^t}$ for D_{Li} and D_{C}.

IV. ERROR ANALYSIS

The statistical error in $\sigma(\Omega_i)$ [Eq. (2)] is given by

$$\Delta\sigma(\Omega_i) = \Delta\sigma_{\text{tr}}(\Omega_i) = \frac{1}{nt}\left[\left[\frac{\Delta R_i}{R_i}\right]^2_{\text{out}} + \left[\frac{\Delta R_i}{R_i}\right]^2_{\text{in}}\right]^{1/2}, \tag{6}$$

where ΔR_i the error in R_i, is

$$(\Delta R_i)^2 = \frac{(\Delta S_i)^2}{KB^2} = \frac{\frac{S_i}{KB}(KB - S_i)}{KB^2}. \tag{7}$$

The individual $\sigma(\Omega_i)$ values are very strongly correlated since almost all the counts in the transmission detectors are due to particles which traverse all the detectors. We used a Monte Carlo simulation technique which

TABLE III. Extrapolated cross sections σ_{ext} with the corrections $\sigma_{K\text{-decay}}$, $\sigma_{\pi\text{-}\mu}$, σ_{A^t}, and the final total cross sections σ_{tot}, as discussed in the text.

Target	p_{lab}(MeV/c)	σ_{ext}(mb)	$\sigma_{K\text{-decay}}$(mb)	$\sigma_{\pi\text{-}\mu}$(mb)	σ_{A^t}(mb)	σ_{tot}(mb)
^{6}Li	490	89.0	10.3	1.0	0.6	77.2
	534	89.0	7.8	0.9	0.6	79.7
	658	91.2	4.1	0.8	0.6	85.7
	716	91.7	3.2	0.8	0.6	87.1
^{12}C	488	186.1	19.4	0.9	0.15	165.6
	531	184.8	14.7	0.8	0.2	169.2
	656	184.6	7.7	0.7	0.2	176.1
	714	185.6	6.0	0.75	0.2	178.7
^{28}Si	488	426.4	41.6	1.4	1.5	381.9
	531	423.8	31.4	1.1	1.5	389.8
	656	414.2	16.5	0.9	1.5	395.3
	714	414.15	12.9	1.05	1.6	398.6
^{40}Ca	488	586.7	57.1	1.7	1.5	526.4
	531	579.6	43.1	1.35	1.5	533.6
	656	558.7	22.6	1.15	1.5	533.4
	714	554.8	17.8	1.4	1.5	534.0
D_{Li}	490	29.25	3.7	0.5	0.15	25.2
	534	30.8	2.8	0.4	0.2	27.7
	658	29.9	1.5	0.4	0.2	28.2
	716	29.6	1.1	0.4	0.2	28.2
D_{C}	488	29.4	3.8	0.5	0.4	25.5
	531	29.6	2.9	0.45	0.4	26.75
	656	29.6	1.5	0.4	0.5	28.1
	714	29.9	1.2	0.4	0.5	28.8

TABLE IV. Summary of systematic errors in the cross sections.

		Uncertainty due to					
Target	p (MeV/c)	K decay (mb)	π-μ (mb)	Solid angle (mb)	Momentum (mb)	Beam (mb)	Fit (mb)
^{6}Li	490	0.52	0.20	0.11	0.30	0.08	0.10
	534	0.39	0.15	0.10	0.13	0.06	0.25
	658	0.20	0.13	0.10	0.13	0.06	0.20
	714	0.16	0.14	0.05	0.20	0.05	0.45
^{12}C	488	0.97	0.32	0.25	0.60	0.25	0.66
	531	0.73	0.25	0.25	0.40	0.20	0.50
	656	0.38	0.20	0.25	0.20	0.15	0.27
	714	0.30	0.21	0.23	0.20	0.15	0.27
^{28}Si	488	2.08	0.91	0.90	1.80	0.75	2.45
	531	1.57	0.55	0.90	1.30	0.65	2.00
	656	0.82	0.45	0.90	0.65	0.65	2.00
	714	0.65	0.49	0.85	0.70	0.55	1.40
^{40}Ca	488	2.85	1.23	1.55	3.30	1.40	4.70
	531	2.16	0.74	1.40	2.00	1.20	1.80
	656	1.13	0.60	1.40	0.91	1.20	3.25
	714	0.89	0.66	1.30	0.80	0.95	1.30
D	488	0.19	0.12	0.02	0.05	0.01	0.15
	531	0.14	0.07	0.02	0.04	0.01	0.05
	656	0.07	0.05	0.02	0.03	0.01	0.10
	714	0.06	0.05	0.01	0.03	0.00	0.05

incorporated the correlations to determine the statistical errors of the extrapolated cross sections, the detailed discussion can be found in [12]. The method gives results which are consistent with the method described in [3]. The systematic errors in the various parameters of the measurement or in the analysis procedure and the statistical errors are shown in Table IV and Table V.

The major systematic error in the total cross section comes from the decay of kaons between the target and the detector array. It is a consequence of the uncertainty in the momentum loss in the target and causes a 5% uncertainty in the K-decay correction. This systematic error was negligible for the ratios. All systematic errors are shown in Table IV.

TABLE V. Summary of total cross sections and ratios measured in this experiment, and their systematic (sys.), statistical (stat.) and total (tot.) errors.

	p	σ	$\Delta\sigma$			Ratio	ΔR_T		
Target	(MeV/c)	(mb)	sys. (mb)	stat. (mb)	tot. (mb)	R_T	sys.	stat.	tot.
^{6}Li	488	77.17	0.65	0.71	0.96	1.016	0.005	0.024	0. 024
	531	79.72	0.52	0.37	0.64	0.979	0.005	0.011	0. 011
	656	85.71	0.36	0.30	0.47	1.015	0.002	0.008	0. 008
	714	87.05	0.54	0.34	0.64	1.013	0.007	0.007	0. 008
^{12}C	488	165.60	1.40	1.08	1.77	1.090	0.010	0.024	0. 026
	531	169.16	1.05	0.58	1.20	1.038	0.005	0.011	0. 011
	656	176.09	0.62	0.43	0.76	1.043	0.005	0.008	0. 009
	714	178.66	0.57	0.44	0.72	1.039	0.003	0.007	0. 008
^{28}Si	488	381.94	3.97	2.72	4.81	1.077	0.014	0.024	0. 028
	531	389.78	3.11	1.05	3.29	1.025	0.007	0.010	0. 013
	656	395.33	2.56	0.79	2.67	1.003	0.008	0.007	0. 011
	714	398.61	2.03	1.00	2.27	0.994	0.004	0.007	0. 008
^{40}Ca	488	526.37	6.86	3.40	7.65	1.039	0.014	0.023	0. 027
	531	533.57	3.98	1.42	4.22	0.983	0.002	0.010	0. 010
	656	533.38	4.05	1.10	4.20	0.947	0.009	0.007	0. 011
	714	534.00	2.48	1.35	2.82	0.932	0.002	0.006	0. 007
D	488	25.33	0.28	0.55	0.61				
	531	27.15	0.17	0.27	0.32				
	656	28.15	0.14	0.20	0.24				
	714	28.65	0.10	0.18	0.20				

The next important systematic error is due to the extrapolation to zero solid angle. We determined the fitting error by repeating the extrapolation (1) by increasing the order of the polynomial by one above the nominal order and (2) by removing the first detector from the fit using the nominal polynomial order. The two modifications compensated each other, i.e., if one of the tests caused the extrapolated cross section to be larger than the nominal result, the other caused it to be smaller. Since both tests are exaggerated modifications, we chose a fitting error which equals half of the larger of the two deviations. The systematic error in the ratios is almost totally due to just the fitting error.

There are also systematic errors in the corrections that were discussed above, in particular, those that depend on momentum. The uncertainty in the momentum at the center of the target is a combination of the error in the determination of the beam momentum (0.25–0.4)%, and the uncertainty in the calculation of the energy loss of the beam on the way to the middle of the target. Most of the energy is lost in the radiator cell of the Cherenkov counter and the rest is lost in the target. Since we know the thickness of the target very well, we are left with the uncertainty in the cell thickness. We estimated an uncertainty of 1 mm in the radiator length corresponding to about 4%, which results in 0.05–0.1% uncertainty in the momentum. Furthermore, we assume a 5% uncertainty in the dE/dx tabulations, which gives a relative error of 0.1–0.25%. The total error in the momentum is listed in Table II. More details are given in Ref. [12]. The beam has a momentum distribution of ±3% FWHM. In order to get the sensitivity of the cross sections to the width of this distribution, we repeated the data analysis for momenta that were larger and smaller by 3% from the nominal one. The results were symmetric around the nominal values. Thus, the width does not contribute to the error.

There is an error in the π, μ correction mentioned above. We estimated an uncertainty of 5% for the π-nucleus cross sections. The resulting systematic error is listed in Table IV.

We took into account the error in the solid angles due to the uncertainty (1 mm) in the distance between the target and the first counter (43.8 cm). Any variations in the spacing between the successive detectors within the array will average out. Another parameter that can affect the solid angle is the effective radius of the detectors. A scintillator inefficiency near the rim would reduce the solid angle. A 1 mm reduction of the radius near the rim would reduce the solid angles of the first and last detectors by 2% and 0.5% change, respectively. The light collection for the small detectors is better than for the larger ones. Therefore, we estimate an overall error of 0.5% for the solid angles for all the detectors. We repeated the analysis by varying all the parameters that depend on the solid angles within the range we just discussed. The overall error in the cross section due to the solid angle uncertainties is the rms convolution of the two.

The fact that the beam is not ideally thin was taken into account in the Coulomb, nuclear-Coulomb, and elastic corrections. We estimated the errors in the cross sections due to uncertainties in the beam parameters (position σ_x, σ_y and angle $\sigma_\theta, \sigma_\phi$) by redoing the analysis where those parameters were increased by 15% of their nominal values. The results appear in Table IV.

As shown in Table V, the systematic errors in the ratios are generally smaller than the statistical errors. This is not true in the separate total cross sections. The experiment was designed to minimize the errors in the ratios and we succeeded in this endeavor.

V. RESULTS AND DISCUSSION

This section presents the final total cross sections and ratios, following the analysis of Secs. III and IV. The results are summarized in Table V.

A. Total cross sections

Figure 3 shows all the measured cross sections, including the earlier data of Bugg *et al.* [14] and Krauss *et al.* [3]. In order to show the nearly constant value of the total cross section per nucleon, we plot that quantity versus A in Fig. 4, for 531 MeV/c. The deviation from a constant is less than 3.4%. This suggests that the low-momentum K^+ is a good hadronic probe capable of penetrating a large part of the nuclear volume.

We see in Fig. 3 that the cross sections for the light nuclei increase with momentum, while for calcium there is only a very weak momentum dependence.

B. Ratio

The measured ratios R_T were published earlier [15] and are displayed in Fig. 5. The solid lines represent the upper bound of the optical-model calculations by Gibbs [16] for R_T for ^{6}Li, ^{28}Si, and ^{40}Ca. We note that the data lie consistently above the predictions and that the momentum dependence is not reproduced by the calculation.

Siegel *et al.* [2] pointed out that nucleon-nucleon correlations with a correlation function $f = 1 - \exp[-(r/r_c)^2]$ and $r_c = 0.7$ fm will lower R_T by 5% at 500 MeV/c and about 2% near 800 MeV/c for ^{12}C. It can be seen in Fig. 5 (the dash-dotted line), that this modification brings the calculated values more in line with the experimental momentum dependence. Unfortunately, the correlation calculations are not yet available for the other nuclei, but we expect the trend to be the same.

The differences between the measured ratios and the calculations (upper lines as discussed in Sec. I) are also given in the third column of Table VI in rms units. The fourth column gives "superratios" defined as the ratios between the measured and the calculated R_T. Averaging these "superratios" over all momenta, in the fifth column, gives some global measure of the medium effect. The averaged "superratio" is small for the loosely bound lithium, large for the denser carbon and silicon nuclei, and is again small for calcium.

We should compare the superratios to theoretical estimates for quark deconfinement in nuclei. For this pur-

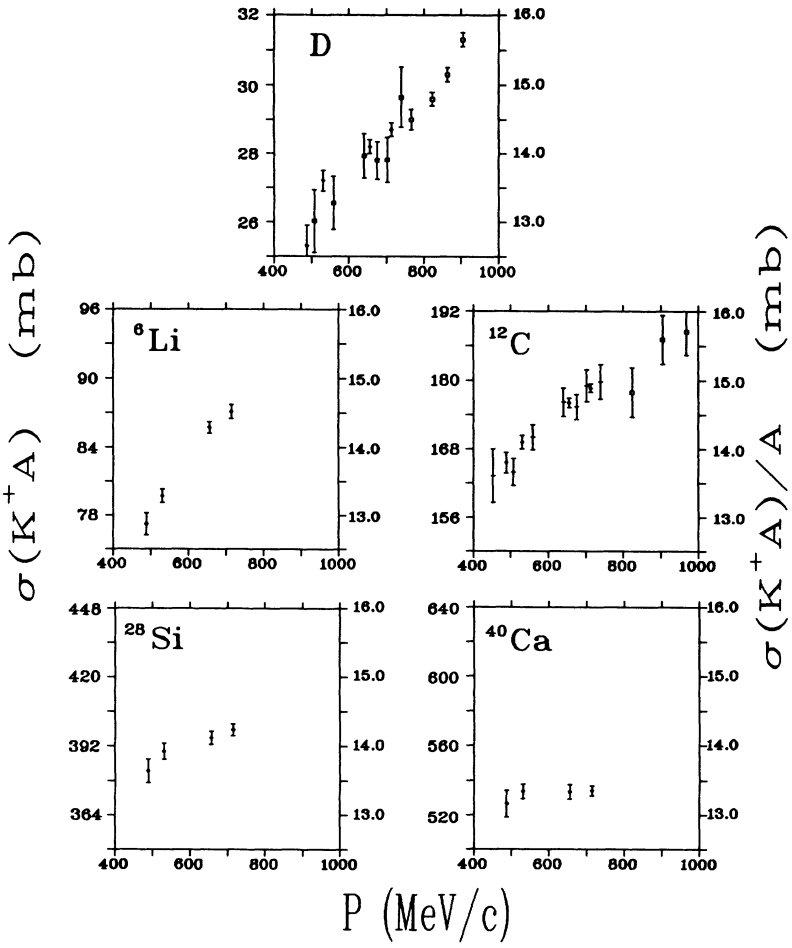

FIG. 3. The total cross section (mb) of K^+ on D, ^{6}Li, ^{12}C, ^{28}Si, and ^{40}Ca as a function of the laboratory momentum. The graphs for the deuteron and the carbon contain data from Krauss *et al.* [3] and Bugg *et al.* [14]. The right-hand vertical scales are the cross sections per nucleon (mb).

pose we use the values of Table I, column (b) of Close *et al.* [17] and Table IV, columns $\tilde{p}_6$ and $\tilde{p}_9$ of Sato *et al.* [18]. They predict a small deconfinement for ^{6}Li (or ^{9}Be) and slowly increasing values up to ^{27}Al after which it stays about constant up to ^{40}Ca. Our data follow this trend for the lighter nuclei. Reference [2] discusses the relation between the S_{11} phase shift and the total cross section. For single scattering in the low-energy limit, the cross section is simply proportional to $\sin^2\delta$. For heavier nuclei, a lesser proportion of the scattering of the kaon is single scattering, and the higher multiple scattering terms become more important. The result is to dilute the effect of an increase in the phase shift, and thus enhance the importance of medium corrections. Without more extensive calculations, as, for example, the inclusion of the effect of pair correlations, our interpretation of the calcium data is only qualitative.

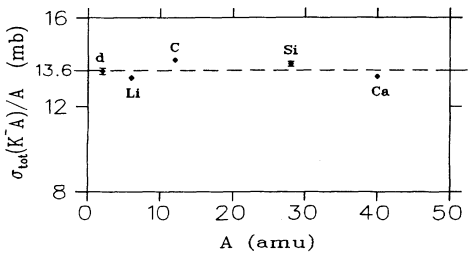

FIG. 4. The total cross section of the K^+ nucleus per nucleon as a function of the mass number for 531 MeV/c and the fit to a constant.

Quantitative comparison of our measured R_T values as a function of momentum, with "nonconventional medium effects" calculations, which were discussed in the introduction, can only be made for ^{12}C. There are no calculations yet for the other nuclei. After publication of the earlier paper, Jiang and Koltun [9] made a detailed calculation of the effect on R_T introduced by meson exchange currents in ^{12}C. They find a momentum-dependent increase in R_T which is below the data, but with a better momentum variation. Calculations for the other nuclei are in progress.

VI. SUMMARY

Previously reported measurements show that the ratio of the K^+ total cross section of C to that of deuterium is substantially above the predictions of published optical-model calculations. These assume that the in-medium scattering amplitude is equal to the free K^+N amplitude, corrected for conventional medium effects. We have extended our measurements of the total K^+ cross sections to targets other than carbon and deuterium. We present cross sections, and ratios of cross sections with respect

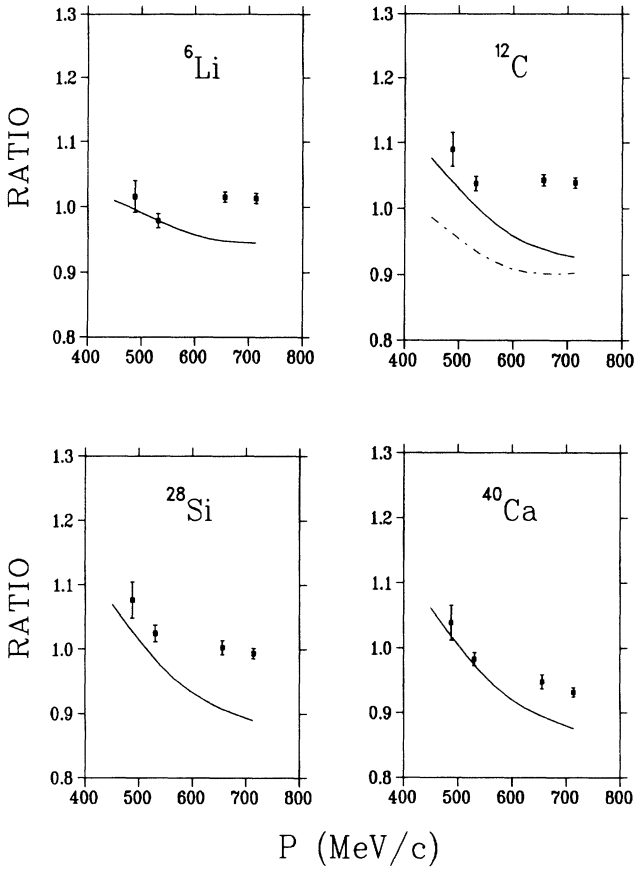

FIG. 5. The experimental ratios along with the theoretical curves that represent the upper limits of the traditional calculations. The effect of the NN correlations in ^{12}C is shown by the dash-dotted line.

to deuterium, of ^{6}Li, ^{12}C, ^{28}Si, and ^{40}Ca. A precision of about 1 % (2% at the lowest momentum) is achieved for the ratios.

A near proportionality of cross section with mass number is demonstrated. This observation establishes the low-momentum kaon as the preferred hadronic probe of nuclear matter.

The new measurements show that carbon is not a unique case. Values of the ratios, R_T, for all measured nuclei are significantly above the upper limits of the calculations mentioned above. The measured ratios are about 10–15 % above the upper limit of the conventional calculation for C and Si, and about 4–5% for both Li and Ca.

Under the assumption that the phenomenon is related to a nuclear medium modification of the K^+-nucleon interaction, the size of the effect is expected to depend on the size of the in-medium amplitude enhancement as well as on the proportion of single scattering to higher-order scattering. In heavier nuclei the latter effect tends to mask the former. This can be seen also in the case of the forward elastic-scattering data of Marlow [19].

Calculations by Siegel *et al.*, assuming an increase in the S_{11} phase shift and folded with the quark deconfinement model [17], predict that the effect will be small for the dilute Li nuclei, largest for C and Si, and slightly smaller for Ca. Other authors have offered alternative calculations for carbon, but with roughly similar results. While no alternative calculations are published for nuclei other than carbon, we presume they would also give similar results.

The measured Li cross sections show only a small enhancement (as expected), while a larger effect is measured for carbon and silicon. The calcium also shows a

TABLE VI. The differences between the measured ratios and the calculations. The third column shows the differences in rms units. The fourth column shows the "superratio" (as described in the text) and the fifth column shows this "superratio" averaged over all momenta.

Target	p (MeV/c)	Standard deviation	R_t(exp.)/R_T(calc.)	Averaged superratio
^{6}Li	488	0.8	1.020	
	531	0.0	1.000	
	656	8.4	1.071	
	714	8.6	1.073	1.054 ± 0.005
^{12}C	488	1.9	1.047	
	531	3.2	1.036	
	656	11.6	1.112	
	714	14.0	1.121	1.094 ± 0.006
^{28}Si	488	1.8	1.048	
	531	3.1	1.042	
	656	8.7	1.106	
	714	13.0	1.118	1.095 ± 0.006
^{40}Ca	488	0.8	1.020	
	531	1.0	1.010	
	656	4.9	1.059	
	714	8.0	1.064	1.044 ± 0.006

small enhancement. The medium corrections referred to above would be expected to be larger in the case of calcium than for the lighter nuclei. This follows from the fact that the proportion of scattering for orders higher than single scattering is largest for calcium. The uncertainty in the medium corrections, as expressed by lower and upper bound values by Siegel *et al.*, is expected to be larger for the heavier nuclei. A comparison to the upper bound for heavy nuclei would thus be less meaningful. This argument, however plausible, is not supported by a detailed calculation; hence we are able to draw only qualitative conclusions with regard to calcium.

The dependence of the measured ratios on kaon momentum for all nuclei appears to be less marked than the model predictions. That fact by itself does not necessarily imply a contradiction with theory. As pointed out in in the paper of Siegel, Kauffman, and Gibbs, some medium corrections, for example, a nucleon pair-correlated repulsion, would lead to a much flatter curve as a function of momentum. In the absence of a specific calculation, we cannot claim that the data cannot be fit by the theory.

Recently, several studies of K^+ nuclear elastic, inelastic, and quasifree scattering have been completed at the Brookhaven AGS. With an improved set of these cross sections, taken in conjunction with the total cross section data, a better understanding of the nature of both the in-medium K^+N interaction and the conventional and unconventional medium effects is anticipated. Further calculations on calcium, silicon, and lithium would also be helpful.

ACKNOWLEDGMENTS

We have benefited greatly from the calculations by W. R. Gibbs, P. B. Siegel, and W. B. Kaufmann, and from discussions with them and with C. B. Dover, A. Gal, and D. Koltun. We would like to thank our colleagues D. Ashery, J. Hiebert, R. R. Johnson, T. Kishimoto, M. A. Moinester, and R. Olshevsky who collaborated in the earlier experiment of K^+ scattering on ^{12}C. We also wish to acknowledge the contributions of our technical staff: J. Rutherford, E. Meier, A. Minn, G. Sheffer, and M. Zilka. This work was performed under the auspices of the U.S. Department of Energy (DE-AC02-76CH00016), and the U. S.–Israel Binational Science Foundation.

[1] C. B. Dover and P. J. Moffa, Phys. Rev. C **16**, 1087 (1977).
[2] P. B. Siegel, W. B. Kaufmann, and W. R. Gibbs, Phys. Rev. C **30**, 1256 (1984); **31**, 2184 (1985).
[3] R. A. Krauss *et al.*, Phys. Rev. C **46**, 655 (1992).
[4] C. M. Chen and D. J. Ernst, Phy. Rev. C **45**, 2019 (1992).
[5] G. E. Brown, C. B. Dover, P. B. Siegel, and W. Weise, Phys. Rev. Lett. **60**, 2723 (1988).
[6] Y. Mardor *et al.*, Phys. Rev. Lett. **65**, 2110 (1990).
[7] J. C. Caillon and J. Labarsouque, Phys. Lett. B **295**, 21 (1992).
[8] S. V. Akulinichev, Phys. Rev. Lett. **68**, 290 (1992).
[9] M. F. Jiang and Daniel S. Koltun, Phys. Rev. C **46**, 2462 (1992).
[10] R. A. Krauss, Ph.D. thesis, Texas A&M University, 1991, unpublished.
[11] Y. Mardor, M.Sc. thesis, Tel Aviv University, 1990, unpublished.
[12] R. Weiss, M.Sc. thesis, Tel Aviv University, 1992, unpublished.
[13] W. B. Kaufmann and W. R. Gibbs, Phys. Rev. C **40**, 1729 (1989).
[14] D. Bugg *et al.*, Phys. Rev. **168**, 1466 (1968).
[15] R. Sawafta *et al.*, Phys. Lett. B **307**, 293 (1993).
[16] W. R. Gibbs, private communication.
[17] F. E. Close, R. L. Jaffe, R. G. Roberts, and G. G. Ross, Phys. Rev. D **31**, 1004 (1985).
[18] M. Sato, S. A. Coon, H. J. Pirner, and J. P. Vary, Phys. Rev. C **33**, 1062 (1986).
[19] D. Marlow *et al.*, Phys. Rev. C **30**, 1662 (1984).